

Modeling and design of 2D photonic crystal based Y type dual band wavelength demultiplexer

R. K. Sinha · Swati Rawal

Received: 28 November 2007 / Accepted: 23 September 2008 / Published online: 6 November 2008
© Springer Science+Business Media, LLC. 2008

Abstract In this paper, photonic bandgap (PBG) induced wave guiding application of photonic crystals is exploited to design Dual Band Wavelength Demultiplexer (DBWD) for separating two telecommunication wavelengths, 1.31 and 1.55 μm . Two designs that use silicon rods in air and embedded air holes in silicon are realized for this purpose. Plane wave expansion (PWE) method and two dimension Finite Difference Time Domain (FDTD) methods are used to design and analyze the DBWD in Y type photonic crystal structure. Numerical analysis indicates that these designs enable the separation of two wavelengths with very high optical power extinction ratios. Other filter parameters like transmittance and quality factor are also calculated to confirm superior performance of the proposed design of photonic crystal based DBWD.

Keywords Photonic crystal · Photonic bandgap materials · Linear defect waveguide · Wavelength demultiplexer

1 Introduction

Photonic crystals (PhCs) introduced by Yablonovitch (1987) have emerged as one of the most significant topics in the field of optical telecommunication. These are defined as materials which have refractive index periodically varying along one, two or three dimension. If the refractive index contrast is sufficiently high, it gives rise to the formation of photonic bandgap (PBG) materials which can realize the localization and trapping of light over a band of frequencies (Joannopolous et al. 1995). By locally breaking the periodicity of

R. K. Sinha · S. Rawal (✉)

Department of Applied Physics, Centre of Relevance and Excellence in Fiber Optics and Optical Communication, Faculty of Technology, Delhi College of Engineering, University of Delhi, Bawana Road, Delhi 110042, India
e-mail: swati.rawal@yahoo.com

R. K. Sinha
e-mail: dr_rk_sinha@yahoo.com

photonic crystal, by creating vacancies or changing the radius of rods/holes, a region with optical properties different from surrounding bulk photonic crystal can be created. This is referred to as PBG optical waveguide (Sakoda 2001) or simply PhC waveguide (WG). Radiation losses exhibited by the PhC sharp bend waveguides are far lesser than conventional waveguides (Valsov and McNab 2004). Two dimension PBG waveguides can be used to design a variety of structures as directional couplers (Nagpal and Sinha 2004), beam splitters (Chen et al. 2004), multiplexers and demultiplexers (Centeno et al. 1999; Tekeste and Yarrison-Rice 2006; Haxha et al. 2005), resonators (Fan et al. 1999), polarizers (Sinha and Kalra 2006a,b), polarization beam splitter (Zabelin et al. 2007) and so on.

In the recent past, interest has been grown in the design and development of DBWD because of their wide applications in bidirectional communication networks (Chien et al. 2004, 2006; Chung and Lee 2007). For example, 1.31/1.55 μm duplex devices are commonly used in fiber-to-the-home (FTTH) transmission systems and are used in the Coarse Wavelength Division Multiplexed (CWDM) systems as well (Fyberdyne Labs 2007). PhCs have opened new possibilities for ultra compact wavelength selective optical devices owing to their PBG induced wave guiding properties. Hence, in the proposed paper wave guiding phenomenon due to PBG property of PhC is exploited for the formation of DBWD in Y type PhC structure, as shown in Figs. 2 and 7. This design of DBWD separates the two telecommunication wavelengths 1.31 and 1.55 μm with a very high extinction ratio and superior quality factor and transmission characteristics. Since the PBG structures strongly control the flow of light, therefore defect created in periodic lattice of PhC results in the confinement of light along specified one arm of the two arms of Y type crystal. Here, we report the design of two structures, one is a hexagonal lattice with silicon rods in air and other is the embedded hexagonal lattice arrangement of air holes in silicon. Both Y type PhC hetrostructures are analyzed using PWE method (Plihal and Maradudin 1991; Villeneuve and Piche 1992) and the performance characteristics in terms of extinction ratio, quality factor and transmittance is obtained by applying 2D FDTD method (Taflove 1998; Yee 1966).

2 Structure design

In the proposed paper we have designed PhC based DBWD having hexagonal lattice of silicon rods in air or embedded air holes in silicon material. The lattice constant and radius of rods or holes were chosen to provide a wide wavelength span (1,250–1,600 nm) at the band edge of input waveguide of DBWD. Selection of lattice constant and radius of rods/holes of the structure is based on the fact that the bandgap exist for both the wavelengths, 1.31 and 1.55 μm so that when line defects are created in photonic crystals, they produce guided modes in photonic crystals corresponding to these wavelengths. Defect radius is chosen such that band gap exist for 1.55 μm in one arm of the Y type DBWD and not for 1.31 μm and vice versa for other arm. Structures having silicon rods in air provide large PBG at technologically convenient geometric parameters with $r/a < 0.5$, as described in Sukanoivanov (2006). However, taking into view practical applications for fabrication, structure having embedded air holes in silicon material is more promising candidate for large scale integration than that of structure having silicon rods in air. Propagation of light is simulated by 2D FDTD method for wavelengths 1.31 and 1.55 μm and it indicates that 1.31/1.55 μm mixed light will be separated into two lights and guided into two output ports of Y type PhC.

2.1 2D PhC wavelength demultiplexer using silicon rods in air

In this section we have designed a 2D PhC slab with hexagonal lattice of Si ($n = 3.42$) rods in air. We first study the photonic bandgap variation using PWE method for Transverse magnetic modes (TM polarization) where the electric field component of electromagnetic waves is oriented perpendicular to the plane of propagation. To obtain PBG for the desired range of wavelength covering both 1.31 and 1.55 μm , we have chosen lattice constant, $a = 0.68 \mu\text{m}$ and rod radius $r = 0.2 \mu\text{m}$. With these parameters PhC provides a large bandgap in range of normalized frequency 0.42318–0.54325 for TM polarization (Fig. 1).

Now, a linear defect waveguide is formed by removing few rods from the direction of propagation. Since the designed structure possesses PBG for TM polarization in the wavelength range $1.25 \mu\text{m} \leq \lambda \leq 1.6 \mu\text{m}$, both wavelengths, 1.31 and 1.55 μm , are guided through the region of input waveguide (Input Wg) as shown in Fig. 3a. Further we design a DBWD by changing the geometrical parameters of Si rods in two arms of Y type photonic bandgap induced waveguides (Fig. 2). Radii of Si rods in one arm of the structure, named Output Wg1, is changed such that signal of 1.55 μm experiences bandgap and 1.31 μm passes through while radii of Si rods in other arm of the structure, named Output WG2, is changed such that signal of 1.31 μm experiences bandgap and 1.55 μm passes through. Figure 3b and c shows that guided modes exist for 1.31 μm in Output Wg1 and 1.55 μm in Output Wg2.

Here we observe that a range of radii exists for which the desired range of bandgap appears. Hence we investigated the defect radius by studying the variation of transmittance in the output ports with defect radius r_d (Fig. 4). 2D FDTD method for TM polarization was utilized to generate data for these plots and that radius is chosen for which transmitted power is maximum.

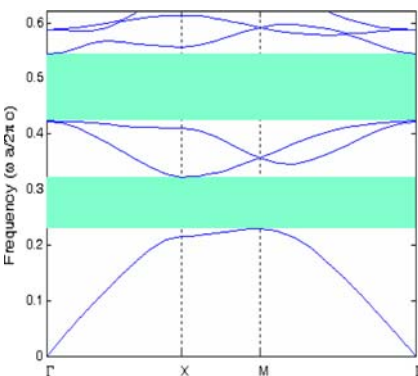


Fig. 1 TM band structure of photonic crystal structure having silicon rods in air, for $r = 0.2 \mu\text{m}$

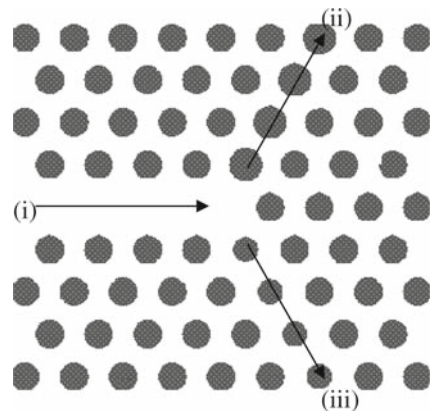


Fig. 2 Schematic diagram of proposed DBWD having silicon rods in air with (i) input Wg, (ii) output Wg1 and (iii) output Wg2

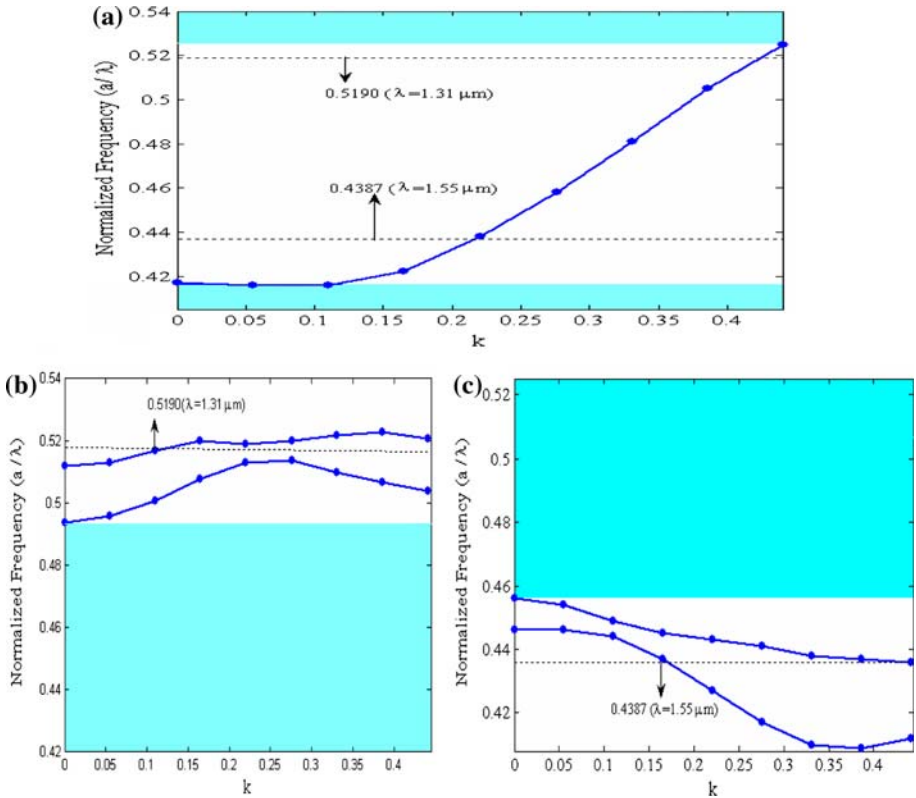


Fig. 3 Dispersion relation of the three involved PhC waveguides. The blue line corresponds to the respective guided modes for TE polarization in **a** input Wg, **b** output Wg1 and **c** output Wg2

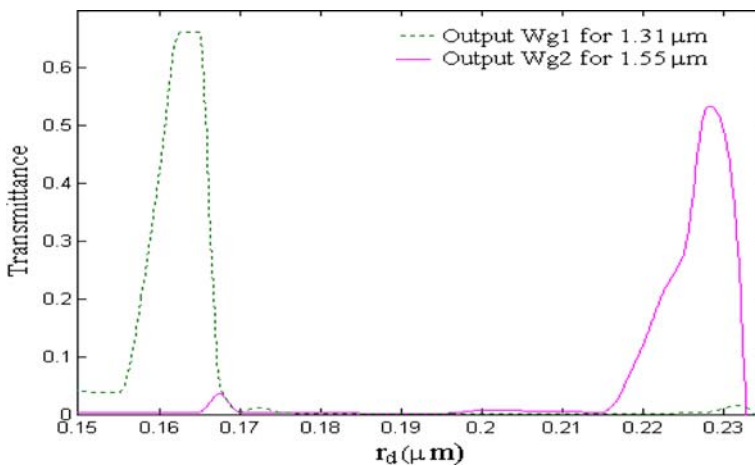


Fig. 4 Variation of transmittance with defect radius r_d in two output waveguides, output Wg1 and output Wg2 for TM polarization of 1.31 and 1.55 μm

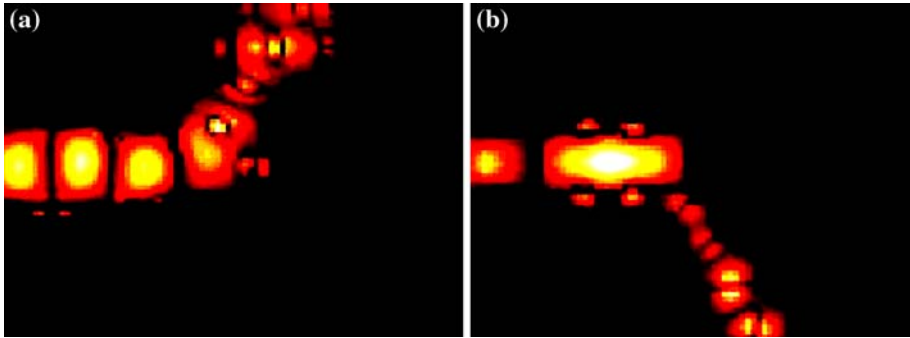


Fig. 5 Field pattern for TM polarization at **a** $\lambda = 1.31 \mu\text{m}$ and **b** $\lambda = 1.55 \mu\text{m}$ for the designed Y type DBWD having silicon rods in air

Note that the maximum efficiency of the device is obtained when defect radius in output Wg1 is $r_d = 0.2318 \mu\text{m}$ for wavelength $1.31 \mu\text{m}$ to pass through and $1.55 \mu\text{m}$ to suffer bandgap. In similar line, the maximum transmission efficiency for wavelength $1.55 \mu\text{m}$ of the device is obtained when defect radius in output Wg2 is $r_d = 0.1768 \mu\text{m}$. The field pattern for TM polarization for the two telecom wavelengths, 1.31 and $1.55 \mu\text{m}$ in Y type DBWD having silicon rods in air is shown in Fig. 5. The type of launch field is Gaussian Continuous Wave (CW). Beam width and step size is taken to be 0.1 and $0.005 \mu\text{m}$. Boundary conditions for 2D FDTD simulation of designed structure is taken as $X(\text{min}) : X(\text{max}) = -5.6525 \mu\text{m} : 5.6525 \mu\text{m}$ & $Z(\text{min}) : Z(\text{max}) = -2.9996 \mu\text{m} : 2.9996 \mu\text{m}$. Output power is determined by the time monitors at output end of two output waveguides. It is observed that $1.31 \mu\text{m}$ is obtained from Output Wg1 having defect radius $r_d = 0.2318$ and $1.55 \mu\text{m}$ is obtained from Output Wg2 having defect radius $r_d = 0.1768 \mu\text{m}$ (Fig. 5).

2.2 2D PhC wavelength demultiplexer using air holes in silicon

The second type of DBWD is designed using silicon material ($n = 3.42$) with embedded hexagonal lattice arrangement of air holes. Lattice constant is chosen to be $a = 0.48 \mu\text{m}$. While studying the photonic bandgap variation using PWE we found that large photonic bandgap in the range $1.25 \mu\text{m} \leq \lambda \leq 1.60 \mu\text{m}$ is obtained for the transverse electric modes (TE polarization) in the hexagonal arrangement of embedded air holes in silicon material. These air holes have radius $r = 0.1896 \mu\text{m}$ (Fig. 6).

Now, we create a linear waveguide in the crystal by removing few holes from the periodic structure so that TE polarization of wavelengths 1.25 – $1.60 \mu\text{m}$ can be guided into the input waveguide, shown as Input Wg in Fig. 7. The PBG based Y type DBWD is then created by changing the geometrical parameters of the air holes in the two arms of Y type photonic bandgap induced waveguides such that wavelength of $1.31 \mu\text{m}$ is obtained at the output end of one of the arms and wavelength of $1.55 \mu\text{m}$ is obtained at the output end of the other arm. Thus radius of the air holes in the two output waveguides are varied such that wavelength $1.55 \mu\text{m}$ experiences bandgap in one arm (output Wg1) of Y type demultiplexer and $1.31 \mu\text{m}$ is guided through it while wavelength $1.31 \mu\text{m}$ experiences bandgap in the other arm (output Wg2) of Y type demultiplexer and $1.55 \mu\text{m}$ passes through it. Figure 8 shows the guided modes for the three involved photonic crystal waveguides.

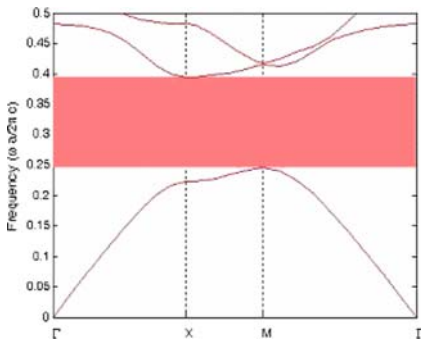


Fig. 6 TE band structure of photonic crystal structure having embedded air holes in silicon for $r = 0.1896 \mu\text{m}$

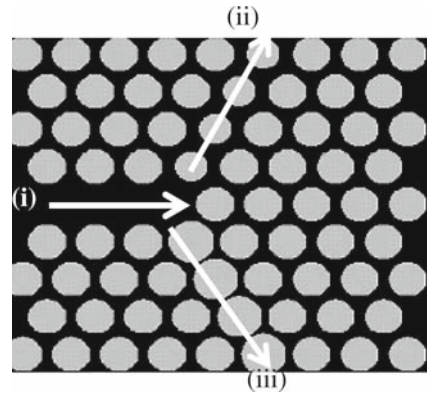


Fig. 7 Schematic diagram of proposed DBWD having embedded air holes in silicon material with (i) input Wg, (ii) output Wg1 and (iii) output Wg2

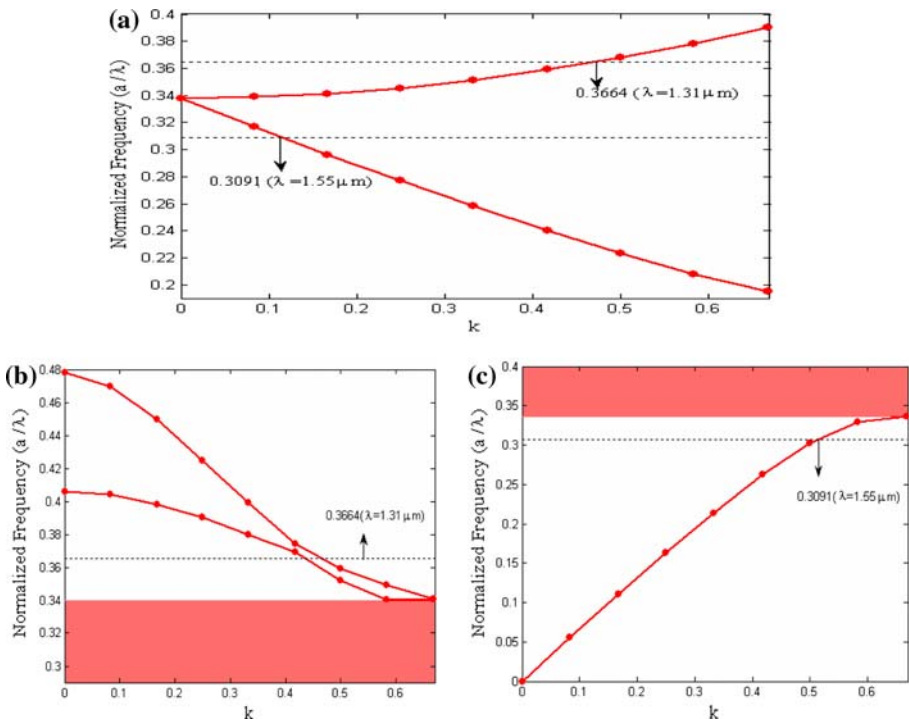


Fig. 8 Dispersion relation of the three involved PhC waveguides. The blue line corresponds to the respective guided modes for TE polarization in **a** input Wg, **b** output Wg1 and **c** output Wg2

Here we observe that while varying the radii to obtain the desired bandgap, a range of radii exists for which the given bandgap appears. We have chosen that radii for which transmitted power is maximum. Hence, we investigated the defect radius by studying its variation with transmittance in the two output ports at 1.31 and 1.55 μm for TE polarization

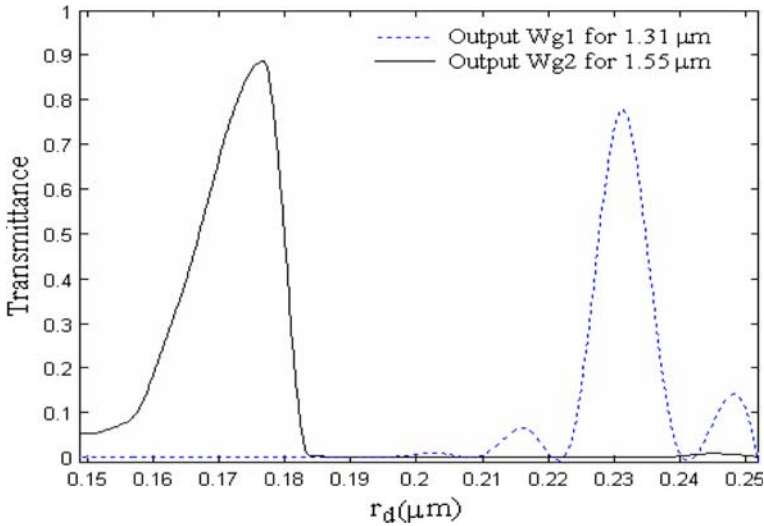


Fig. 9 Variation of transmittance with defect radius r_d in two output waveguides, output Wg1 and output Wg2 for TE polarization of 1.31 and 1.55 μm

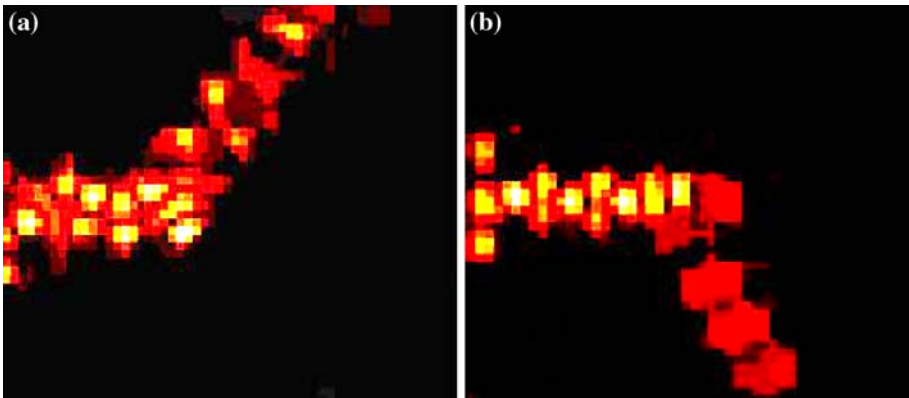


Fig. 10 Field pattern for TM polarization at $\lambda = 1.31 \mu\text{m}$ and $\lambda = 1.55 \mu\text{m}$ for the designed Y type DBWD having embedded air holes in silicon material

(Fig. 9). It is noted that maximum efficiency for 1.31 guidance is obtained when defect radius is $r_d = 0.1646 \mu\text{m}$ in output Wg1 while maximum efficiency of 1.55 μm is obtained when defect radius is $r_d = 0.228 \mu\text{m}$ in Output Wg2. The field pattern for TE polarization for the two telecom wavelengths, 1.31 and 1.55 μm in Y type DBWD having embedded air holes in silicon material is shown in Fig. 10. The type of launch field is Gaussian Continuous Wave (CW). Beam width and step size is taken to be 0.1 and 0.00025 μm . Boundary conditions for 2D FDTD simulation of embedded air hole type DBWD is taken as $X(\text{min}): X(\text{max}) = -2.6775 \mu\text{m}: 2.6775 \mu\text{m}$ & $Z(\text{min}): Z(\text{max}) = -2.9894 \mu\text{m}: 2.9894 \mu\text{m}$. Output power is determined by the time monitors at output end of two output waveguides. It is observed that 1.31 μm is obtained from Output Wg1 having defect radius $r_d = 0.1646$ and 1.55 μm is obtained from Output Wg2 having defect radius $r_d = 0.228 \mu\text{m}$ (Fig. 10).

3 Numerical analysis

The proposed Y type DBWD is simulated using 2D FDTD method. Output Wg1 reflects the radiation with wavelength $1.55\ \mu\text{m}$ and Output Wg2 reflects the radiation with wavelength $1.31\ \mu\text{m}$. Efficiency of the device in both type of structure (i.e. for silicon rods in air and embedded air holes in silicon) was investigated by calculating different filter parameters like transmittance, extinction ratio and quality factor.

3.1 Transmittance

Transmittance of the designed DBWD is defined as the ratio of output intensity (I_{out}) from either of the two output waveguides to the incident intensity (I_{in}) at the entrance of the Y type waveguide:

$$T = \frac{I_{\text{out}}}{I_{\text{in}}}$$

Variation of transmittance from the two output waveguides of Y type PhC structure consisting of silicon rods in air-based DBWD is shown in Fig. 11a and for air holes in silicon-based DBWD is shown in Fig. 11b. It can be noted from the two graphs that maximum efficiency in output Wg1 is shown for wavelength $1.31\ \mu\text{m}$ and in output Wg2 is shown for $1.55\ \mu\text{m}$. Hence the two telecommunication wavelengths 1.31 and $1.55\ \mu\text{m}$ can be separated out easily using these two designs of DBWD.

3.2 Extinction ratio

Further we calculate extinction ratios ER1 and ER2 of the DBWD which explains that separation of two wavelengths, 1.31 and $1.55\ \mu\text{m}$ is achieved. The extinction ratios ER1 and ER2 are defined as

$$\text{ER1} = 10 \log_{10} \frac{\text{fractional output power for } 1.31\ \mu\text{m wavelength in waveguide1}}{\text{fractional output power for } 1.31\ \mu\text{m wavelength in waveguide2}}$$

and

$$\text{ER2} = 10 \log_{10} \frac{\text{fractional output power of } 1.55\ \mu\text{m wavelength in waveguide2}}{\text{fractional output power of } 1.55\ \mu\text{m wavelength in waveguide1}}$$

Simulation by 2D FDTD method indicates that in case of silicon rods in air-based DBWD extinction ratios are $\text{ER1} = 36.30\ \text{dB}$ and $\text{ER2} = 30.40\ \text{dB}$ while in case of air holes in silicon-based DBWD extinction ratios are 22.05 and $22.70\ \text{dB}$ for the two wavelengths, 1.31 and $1.55\ \mu\text{m}$.

The PBG induced DBWDs thus have high extinction ratio for filtering two telecom wavelengths, 1.31 and $1.55\ \mu\text{m}$ efficiently (Wang et al. 2005; Chung and Lee 2007).

3.3 Quality factor

Quality factor is defined as ratio of wavelength at peak transmission λ_0 to full width at half maximum intensity (FWHM) or $\Delta\lambda$

$$Q = \frac{\lambda_0}{\Delta\lambda}$$

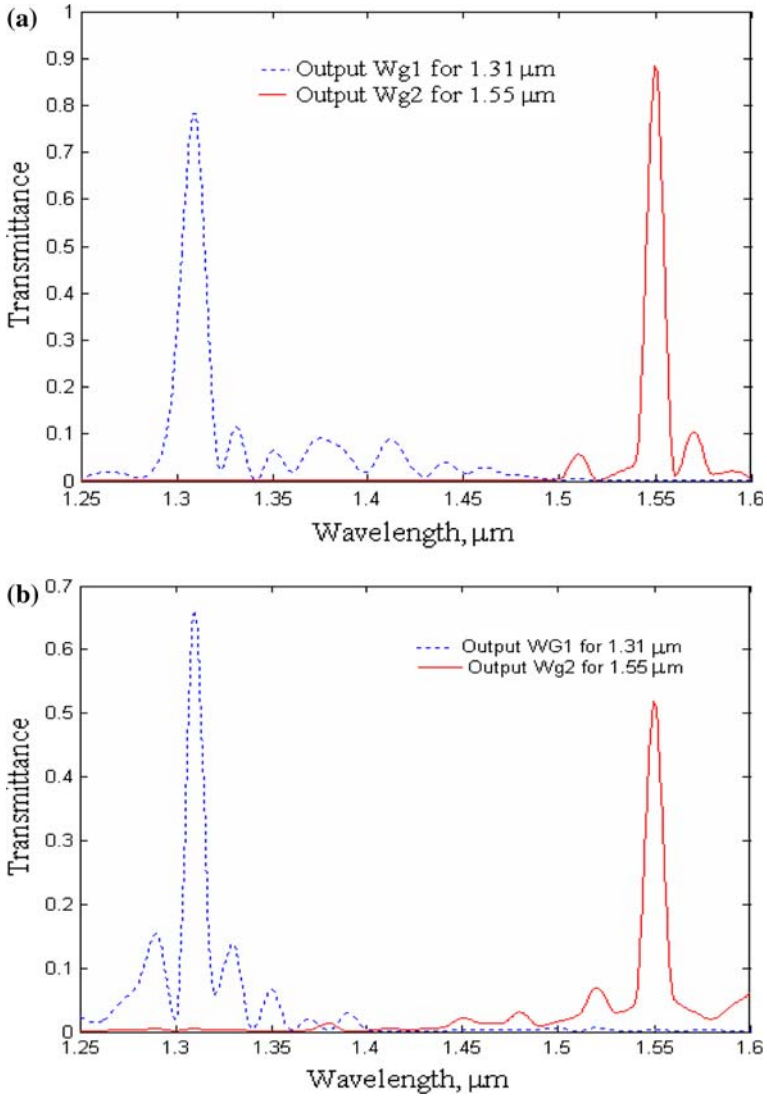


Fig. 11 Variation of transmittance with wavelength at the output end of each output waveguide for **a** the silicon rods in air-based DBWD and **b** air holes in silicon-based DBWD

Quality factor for wavelength 1.31 and 1.55 μm, in case of silicon rods in air-based DBWD is 109.16 and 172.22 while in case of air holes in silicon-based DBWD it is given as 131.0 and 155.0, at the output end of two output waveguides. It is mentioned that these values of quality factors are significantly high at two widely used telecommunication wavelength windows and hence these designs of PhC based DBWD are having superior filter characteristics.

4 Conclusion

In the proposed paper, we have designed photonic crystal based Y type DBWD for two telecommunication wavelengths, 1.31 and 1.55 μm, in PhC employing (i) silicon rods in

air and (ii) embedded air holes in silicon material. Designs of appropriate structures were obtained using PWE method while transmission and other filter characteristics were investigated using 2D FDTD method. It has been demonstrated that the PhC consisting of silicon rods in air-based DBWD reported in this paper exhibit high extinction ratio of 36.30 dB for wavelength 1.31 μm and 30.40 dB for wavelength 1.55 μm . Similarly the other PhC structure i.e. embedded air holes in silicon based DBWD exhibits 22.05 and 22.70 dB for wavelength 1.31 and 1.55 μm respectively. The proposed design also exhibit superior transmittance and high quality factor at these widely used telecommunication wavelengths. Thus the proposed DBWD consisting PhC structure can be effectively used in bidirectional optical transmission systems and networks covering broad spectrum of optical communication windows.

Acknowledgements The authors gratefully acknowledge the initiatives and support towards establishment of “TIFAC Centre of Relevance and Excellence in Fiber Optics and Optical Communication at Delhi College of Engineering, Delhi” through “Mission REACH” program of Technology Vision-2020, Government of India.

References

- Centeno, E., Guizal, B., Felbacq, D.: Multiplexing and demultiplexing with photonic crystals. *Pure Appl. Opt.* **1**, 10–13 (1999). doi:[10.1088/1464-4258/1/5/103](https://doi.org/10.1088/1464-4258/1/5/103)
- Chen, C.C., Chien, H.D., Luan, P.G.: Photonic crystal beam splitters. *Appl. Opt.* **43**, 6188–6190 (2004)
- Chien, F.S.-S., Hsu, Y.J., Hsieh, W.F., Cheng, S.-C.: Dual wavelength demultiplexing by coupling and decoupling of photonic crystal waveguides. *Opt. Express* **12**, 1119–1125 (2004). doi:[10.1364/OPEX.12.001119](https://doi.org/10.1364/OPEX.12.001119)
- Chien, F.S.-S., Cheng, S.-C., Hsu, Y.-J., Hsieh, W.-F.: Dual-band multiplexer/demultiplexer with photonic-crystal-waveguide couplers for bidirectional communications. *Opt. Commun.* **266**, 592–597 (2006). doi:[10.1016/j.optcom.2006.05.055](https://doi.org/10.1016/j.optcom.2006.05.055)
- Chung, L.-W., Lee, S.-L.: Photonic crystal based dual-band demultiplexers on silicon materials. *Opt. Quant. Electron.* **39**, 677–686 (2007). doi:[10.1007/s11082-007-9118-0](https://doi.org/10.1007/s11082-007-9118-0)
- Fan, S., Villeneuve, P.R., Joannopolous, J.D.: Theoretical analysis of channel drop tunneling processes. *Phys. Rev. B.* **59**, 15882–15892 (1999). doi:[10.1103/PhysRevB.59.15882](https://doi.org/10.1103/PhysRevB.59.15882)
- Fyberdyne Labs. <http://www.fiberdyne.com/products/pdf/cwdmintro.PDF>. Cited 11 Sept 2007 (2007)
- Haxha, S., Belhadj, W., AbdelMalek, F., Bouchriha, H.: Analysis of wavelength demultiplexer based on photonic crystals. *Optoelectronics* **152**, 193–198 (2005). doi:[10.1049/ip-opt:20050003](https://doi.org/10.1049/ip-opt:20050003)
- Joannopolous, J.D., Meade, R.D., Winn, J.N.: *Photonic Crystals: Molding the Flow of Light*. Princeton University Press, Princeton (1995)
- Nagpal, Y., Sinha, R.K.: Modeling of photonic bandgap directional couplers. *Microw. Opt. Technol. Lett.* **43**, 47–50 (2004). doi:[10.1002/mop.20371](https://doi.org/10.1002/mop.20371)
- Plihal, M., Maradudin, A.A.: Photonic band structures of two dimensional systems—the triangular lattice. *Phys. Rev. B* **44**, 1865–8571 (1991). doi:[10.1103/PhysRevB.44.8565](https://doi.org/10.1103/PhysRevB.44.8565)
- Sakoda, K.: *Optical properties of photonic crystals*. Springer Series, New York (2001)
- Sinha, R.K., Kalra, Y.: Design of photonic bandgap polarizer. *Opt. Eng. Lett.* **45**, 110503–110505 (2006a)
- Sinha, R.K., Kalra, Y.: Design of optical waveguide polarizer using photonic bandgap. *Opt. Express* **14**, 10790–10794 (2006b). doi:[10.1364/OE.14.010790](https://doi.org/10.1364/OE.14.010790)
- Sukhoivanov, I.A., Guryev, I.V., Shulika, O.V., Kublyk, A.V., Mashoshina, O.V., Alvarado-Mendez, E., Andrade-Lucio, J.A.: Design of the photonic crystal demultiplexers for ultra-short optical pulses using the gap-maps analysis. *J. Optoelectron. Adv. Mater.* **8**, 1622–1626 (2006).
- Taflove, A.: *Advances in Computational Electrodynamics—The Finite Difference Time Domain Method*. Artech House, Norwood (1998)
- Tekeste, M.Y., Yarrison-Rice, J.M.: High efficiency photonic crystal based wavelength demultiplexer. *Opt. Express* **14**, 7931–7942 (2006). doi:[10.1364/OE.14.007931](https://doi.org/10.1364/OE.14.007931)
- Valsov, Y., McNab, S.: Losses in single mode silicon-on-insulator strip waveguides and bends. *Opt. Express* **12**, 1622–1631 (2004). doi:[10.1364/OPEX.12.001622](https://doi.org/10.1364/OPEX.12.001622)
- Villeneuve, P.R., Piche, M.: Photonic bandgaps in two dimensional square lattices-square and circular rods. *Phys. Rev. B* **46**, 4973–4975 (1992). doi:[10.1103/PhysRevB.46.4973](https://doi.org/10.1103/PhysRevB.46.4973)
- Wang, W.K., Wang, S.J., Chen, C.C., Wu, Y.H., Huang, F.H., Chan, Y.J.: 1.3/1.55 μm optical directional coupler by photonic crystal with a defect shifting design. In: *Proceedings of IEEE Conference on Nanotechnology*, Nagoya, Japan, July (2005)

- Yablonovitch, E.: Inhibited spontaneous emission in solid state physics and electronics. *Phys. Rev. Lett.* **58**, 2059–2062 (1987). doi:[10.1103/PhysRevLett.58.2059](https://doi.org/10.1103/PhysRevLett.58.2059)
- Yee, K.S.: Numerical solution of initial boundary value problems involving Maxwell's equations in isotropic media. *IEEE Trans. Antenna Propag.* **14**, 302–307 (1966). doi:[10.1109/TAP.1966.1138693](https://doi.org/10.1109/TAP.1966.1138693)
- Zabelin, V., Dunbar, L.A., Le Thomas, N., Houdre, R.: Self-collimating photonic crystal polarization beam splitter. *Opt. Lett.* **32**, 530–532 (2007). doi:[10.1364/OL.32.000530](https://doi.org/10.1364/OL.32.000530)